DIRECTIONAL CREEP BEHAVIOUR OF TWO MAGNESIUM ALLOY BASE COMPOSITES WITH FIBRES

KAREL MILIČKA*, FERDINAND DOBEŠ

Institute of Physics of Materials, Academy of Sciences of the Czech Republic, Žižkova 22, 616 62 Brno, Czech Republic

Received 14 October 2004, accepted 10 November 2004

Compressive creep behaviour of two composites with magnesium alloy AS21 matrix reinforced by short fibres and short fibres&coarse SiC particles was investigated with the aim to show the influence of the orientation of stress axis to the planar distribution of fibres in the composites. Experiments were performed at 523 K. Strong dependence of time to rupture and minimum creep rate on this orientation were observed in both composites. Stress sensitivity parameters of the minimum creep rate and the time to rupture do not probably depend on the orientation of acting stress to planar fibre distribution in the composites. A specific form of the creep rupture pattern of specimens was observed and is briefly discussed.

K e y w o r d s: creep, metal matrix composites, magnesium alloy, reinforcing fibres

1. Introduction

Recently, a great effort has been paid to explanation of physical aspects of the creep behaviour of metal matrix composites (MMC's) with a distribution of reinforcing short fibres. Most these investigations have been based on the threshold stress concept, e.g. [1–5]. However, these investigations did not consider the crucial fact that structure of such composites is usually not isotropic; the fibres are always in some extent ordered in the volume. As typical examples of such MMC's, the widely used magnesium or aluminium alloy based composites with fibre or hybrid preforms, prepared by squeeze casting, can be considered. Original semi-ordering of fibres into the random planar distribution remains saved also in the final products. Due to ordering of the fibre distribution, most mechanical properties should differ in various geometrical directions of the final product. Trojanová et al. [6] observed

*corresponding author, e-mail: milicka@ipm.cz

an enhanced influence of two basic specimen orientations, i.e., perpendicular or parallel to the fibre planar distribution, i.e., parallel and perpendicular on some mechanical properties of MMC's with QE22 matrices at room temperature. The anisotropy of the MMC's structure influences also their other properties, e.g., heat conductivity [7] or abrasion properties [8].

Up to now, only several papers, e.g. [9–11], have dealt with this influence on creep behaviour. Moreover, only the behaviour in three main directions related to the shape of fibre preform was investigated. However, the knowledge of a more detailed influence of the structure anisotropy on creep characteristics could be very useful for any verification of various up to now suggested models of deformation of this type of MMC's. Results documenting the influence of the stress axis orientation to the plane of fibre distribution on creep properties of two MMC's with a magnesium alloy AS21 are briefly summarized in the present paper.

2. Experimental

Two composites were prepared for experiments. The chemical composition of the matrix magnesium alloy AS21 was (in wt.%): 2.2 Al, 1.0 Si, 0.1 Mn and Mg balanced. Composites were prepared by squeeze casting in the Zentrum für Funktionswerkstoffe, Clausthal-Zellerfeld, Germany. A fibre preform with nominal content of 25 vol.% of Saffil fibres was used in the first composite (in what follows AS21_F). The second composite (AS21_H) contained a hybrid preform with nominally 5 vol.% of Saffil fibres and 15 vol.% of coarse particles of SiC. The cast blocks had roughly parallelepiped shape with dimensions approximately 50 × 90 × 90 mm. Both preforms had a shape of rectangular parallelepiped 25 × 70 × 70 mm and were situated at the centre of the bottom of the blocks (see scheme in Fig. 1).

Fibre preform in AS21_F consisted of planar randomly distributed δ-alumina fibres. The average diameter and length were 3 μm and up to 150 μm, respectively. The light micrographs illustrating structure of the composite in three main planar sections of the preform are shown in Fig. 2. Structures in section planes XZ and YZ are practically identical – the axes of fibres are preferentially coplanar to XY plane or contain only small angles with this plane. In the plane XY, the random distribution of fibres is apparent.

The structure of composite AS21_H in main three planes of the preform is illustrated in Fig. 3. Qualitatively, the distribution of alumina fibres is very similar to their distribution in the composite AS21_F, i.e., typically the preferential planar distribution. The average length of fibres was up to 120 μm and their average diameter was approx. 3 μm. Added coarse SiC particles are relatively homogeneously distributed. Their size was up to 10 μm.

Squeeze – cast blocks of both composites were not subjected to a further heat treatment procedure before creep testing.

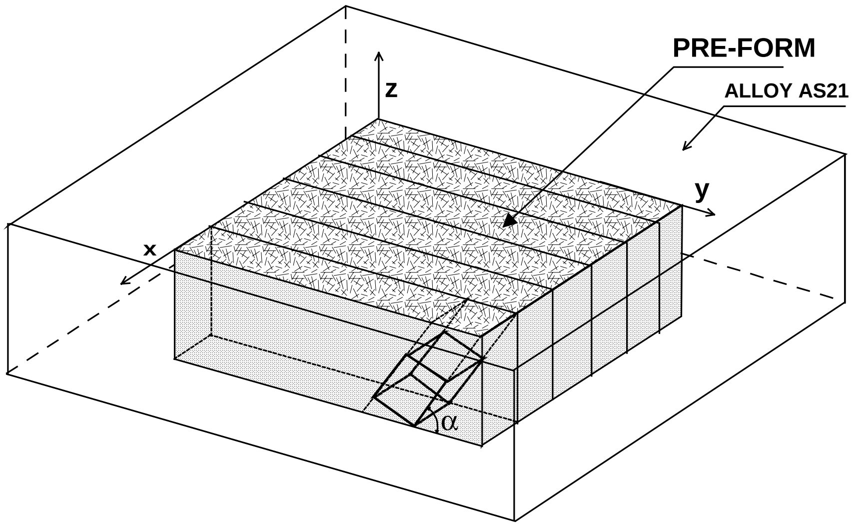

Fig. 1. Scheme of the composite products and the procedure of specimen choice.

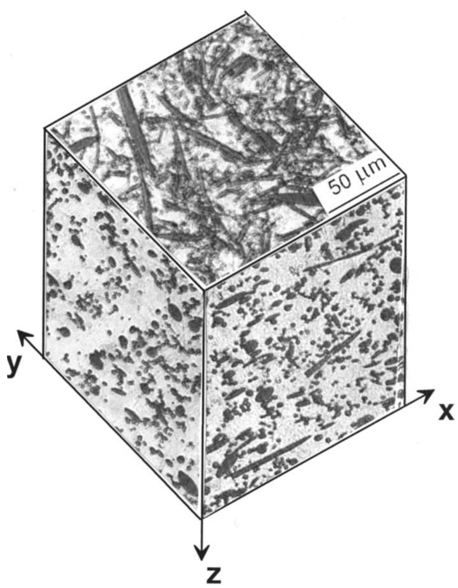

Fig. 2. Structure of the composite AS21_F in three main planes of the preform.

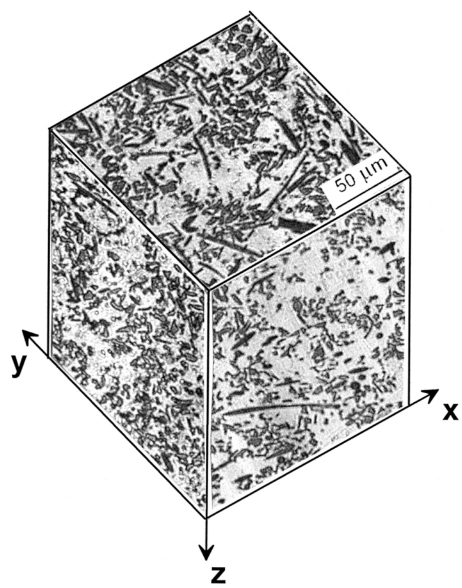

Fig. 3. Structure of the composite AS21_H in three main planes of the preform.

The procedure of specimen choice from the composite volume is apparent from Fig. 1. The ingots were cut parallel to the plane YZ into parts of 7 mm thickness. Obtained parallelepipeds were spark-cut under chosen angles α into semi-products with cross-section 7×7 mm. Consequently, final specimens were manufactured in the parallelepiped form with dimensions $6 \times 6 \times 12$ mm. The last procedure of specimen surfaces preparation was fine grinding and polishing by diamond paste. This procedure allowed metallographic revisions of quality of fibre distribution in the specimen before testing.

Constant stress compressive creep tests of both composites were performed in a protective atmosphere of dried and purified argon. A uniform temperature regime was maintained before the start of each test. During the test, temperature was kept constant within 1 K. The sensitivity of strain measurements was better than 10^{-6} and creep curves were PC recorded. All experiments were performed at 523 K.

3. Results and discussion

3.1 Creep curves

Examples of creep curves for AS21_F and AS21_H composites are plotted in two different coordinate systems in Figs. 4 and 5. The curves of both composites did not differ. Typically, each of the creep curves had usual three stages of creep. The primary stage was always very short; it did not overreach a level of 5 percent of true creep strain ε. The secondary stage with a very short region of the minimum creep rate $\dot{\varepsilon}_{\min}$ was observed on each curve. The relatively long tertiary creep was – as a

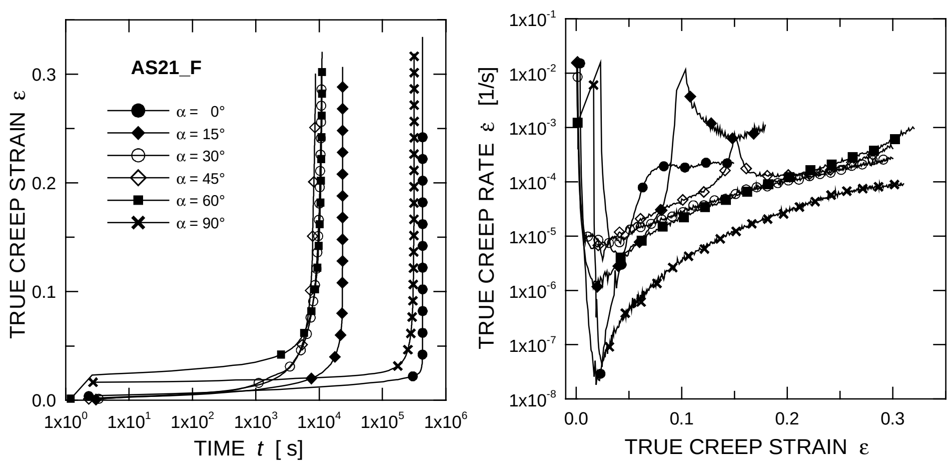

Fig. 4. Examples of creep curves of the composite AS21_F.

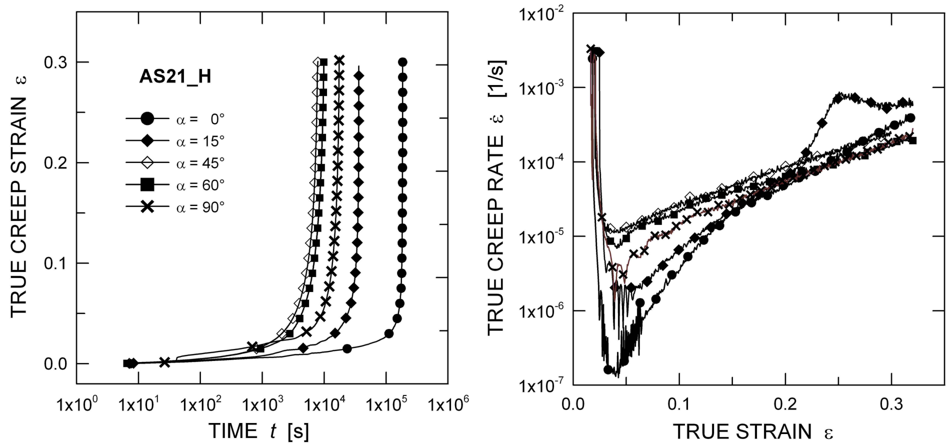

Fig. 5. Examples of creep curves of the composite AS21_H.

rule – finished by a destruction of the specimen into several connected macro-blocks (see paragraph 3.4). At limiting true strain of the used creep machine ($\varepsilon \approx 0.32$), all specimens were destroyed and corresponding time to rupture could be determined from the curves. Irregular progression of the dependences $\dot{\varepsilon}_{\min}$ *versus* ε (local accelerations and consequent strain retardations) observed in some creep curves – are probably due to discontinuous straining processes of the composites. In the vicinity of the minimum creep region, a "jerky" creep was frequently observed. Such phenomenon should detect the start of a specific type of the fracture. However, all these effects necessitate more detailed and complex investigation including detailed observations of corresponding structure development.

3.2 Creep behaviour of the composite AS21_F

The influence of the specimen orientation on creep parameters, i.e., on the minimum creep rate $\dot{\varepsilon}_{\min}$ and time to rupture t_r, is apparent from the Fig. 6. The strong influence of the angle α on both these parameters is apparent. The minimum creep strength corresponds to the angle $\alpha = 45°$. At this angle, the rate $\dot{\varepsilon}_{\min}$ and the time t_r are approximately up to two orders in magnitude greater or smaller, respectively, than values for the angle $\alpha = 0°$ under chosen creep conditions. No simple explanation of such effect can be suggested without detailed knowledge of deformation mechanisms controlling creep of the composite. Any suggestion should take into account the fact, that the final creep behaviour of the composite is determined by a complex of strengthening interactions of the matrix alloy with precipitating particles of secondary phases and with the supplemental reinforcing

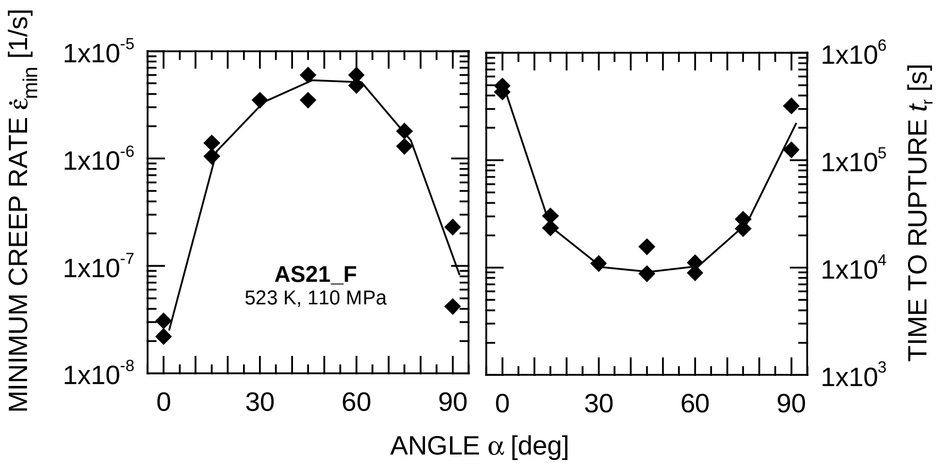

Fig. 6. Orientation dependence of the creep parameters – composite AS21_F.

influence of fibers. However, the dominant influence of fiber distribution is quite beyond dispute in this composite. The strengthening effect of precipitated particles does probably not depend on the orientation of the specimen. The influence of the fibre reinforcement on creep characteristics of the composite AS21_F was discussed in detail elsewhere [12].

3.3 Creep behaviour of the composite AS21_H

Dependences of the rate $\dot{\varepsilon}_{\mathrm{min}}$ and time to rupture t_{r} on the angle α obtained in the composite AS21_H under identical creep conditions, i.e., $T = 523$ K and stress $\sigma = 110$ MPa, are shown in Fig. 7. A strong dependence of both parameters on the angle α has been obtained also in this type of the composite. However, the courses of the dependences differ from those obtained in the composite AS21_F. While the dependences of both parameters were rather symmetrical with respect to an axis $\alpha = 45°$ in the composite AS21_F, these dependences are not so strong in the interval of angles α greater than 45° in the hybrid composite AS21_H. Probably, the relatively small fiber content in the composite has a not so great reinforcing influence at these angles. The strengthening effect of coarse particles of SiC can also contribute substantially to the creep resistance of the composite; this effect should be independent of the angle α. However, the strengthening contribution of SiC particles does not fully compensate the lowered content of fibres in the composite AS21_H (compare dashed poly-lines).

For an explanation of possible mechanisms acting in creep, a knowledge of the activation parameters of creep resulting from the temperature and applied

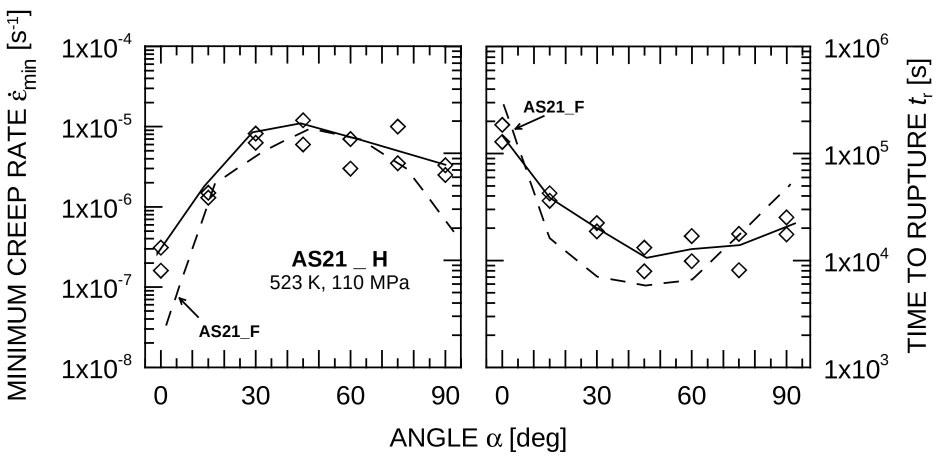

Fig. 7. Orientation dependence of the creep parameters – composite AS21_H.

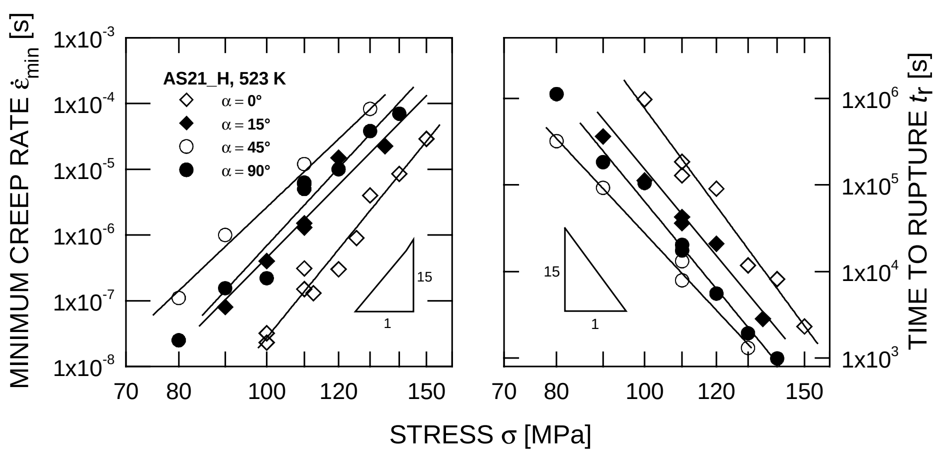

Fig. 8. Stress dependences of the minimum creep rate and time to rupture for various angles α – composite AS21_H.

stress dependences of the minimum creep rate $\dot{\varepsilon}_{\min}$ and time t_r is necessary. From this point of view, the influence of the orientation on these activation parameters should be also very useful in any consideration. The applied stress dependences of the minimum creep rate $\dot{\varepsilon}_{\min}$ and time t_r for various values of the angle α for the composite AS21_H were only examined in the present paper. Both these dependences are plotted in Fig. 8. Straight lines can be drawn through the experimental points in the coordinate log-log system. This implies that the applied stress dependences of the rate $\dot{\varepsilon}_{\min}$ and time t_r can be well described by a power Norton relation. Therefore, the stress sensitivity parameters n and n_r, which are defined as

$$n = (\delta \ln \dot{\varepsilon}_{\min} / \delta \ln \sigma)_T \text{ and } n_r = -(\delta \ln t_r / \delta \ln \sigma)_T,$$

do not depend on the applied stress in the experimental interval; both are determined by the slope of drawn straight lines. Apparently, both parameters probably do not depend on the angle α. Both parameters reach relatively very high values – approximately 15. None of as yet suggested models of creep in MMC's assumes such high values of the parameter n. On the other hand, the fact that the parameters n and n_r do not probably depend on the angle α could be considered the support of identical mechanism of creep at any α. Similar consideration should support also a suggestion of identical mechanisms of rupture (identical n_r).

3.4 Morphology of the ruptured specimens

The shapes of ruptured specimens of the composite AS21_F with different orientations of the axes are illustrated in Fig. 9. The macro-appearance of all ruptured specimens is very similar at all angles α; there are two typical features of the rupture. First, it can be seen that the rupture process does not probably expand along the planes of fibre distribution but predominantly along the planes of maximum shear stress. Apparently, massive macro-slip of specimen parts has occurred predominantly along these or parallel planes. Second, all these "slip planes" are perpendicular to one of the opposite pairs of sides of the specimen parallelepiped (front sides of the specimens in Fig. 9). Naturally, there is a question, how these "slip planes" are oriented to the basic planes of the composite connected with the preform (Fig. 1). A detailed metallographic observation has shown that all these planes are parallel or nearly-parallel to the coordinate X or Y. It means that rupture expansion must go across the planar fibre distribution in all ruptured specimen. An exception is the angle $\alpha = 45°$. In this case, there is a parallelism of the planes of fibre distribution and maximum shear stress in the specimen.

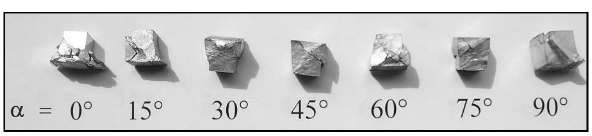

Fig. 9. Shapes of the ruptured specimens with various angles α – composite AS21_F.

Identical conclusions concerning the morphology of ruptured specimens were obtained in both composites investigated. Again, the "slip planes" or "slip directions" go across the planar fibre distribution.

4. Conclusions

From the present study of the influence of orientation between the acting stress and the quasi-planar distribution of reinforcing fibres in the investigated composites with different preform following conclusions can be drawn:

– There is a strong dependence of the creep resistance on the angle α characterizing the stress axis orientation to the planar distribution of fibres in both materials investigated;

– Maximum creep resistance is observed if the stress acts parallel with the planes of fibre distribution ($\alpha = 0°$);

– Minimum creep resistance corresponds to the angle $\alpha = 45°$ in both investigated composites;

– Creep resistance of the composite with fibres is only at $\alpha = 90°$ slightly lower than that at $\alpha = 0°$;

– Creep resistance of the composite with hybrid preform is rather constant at angle $\alpha > 45°$;

– Stress sensitivity parameters n and n_r of the minimum creep rate and time to rupture, respectively, do not probably depend on the angle α;

– Creep rupture of specimens expands across planes of distributed fibres at all angles α.

Acknowledgements

The financial support of the Grant Agency of the Czech Republic within grant 106/03/0843 is gratefully acknowledged.

REFERENCES

[1] LI, Y.—LANGDON, T. G.: Met. Mat. Trans., *A30*, 1999, p. 2059.
[2] KUCHAŘOVÁ, K.—ČADEK, J.: Kovove Mater., *40,* 2002, p. 69.
[3] ČADEK, J.—KUCHAŘOVÁ, K.: Kovove Mater., *41,* 2003, p. 127.
[4] ČADEK, J.—KUCHAŘOVÁ, K.: Kovove Mater., *42,* 2004, p. 9.
[5] ČADEK, J.—KUCHAŘOVÁ, K.—MILIČKA, K.: J. Alloys Comp., *378,* 2004, p. 123.
[6] TROJANOVÁ, Z.—JÄGER, A.—DROZD, Z.: Kovove Mater., *42*, 2004, p. 214.
[7] BARTA, S.—DIEŠKA, P.: Kovove Mater., *41*, 2003, p. 223.
[8] ŠEBO, P.: Kovove Mater., *41*, 2003, p. 248.
[9] PHILLIPS, J.—STAUBACH, M.—SKROTZKI, B.—EGGELER, G.: Mater. Sci. Eng., *A234–236*, 1997, p. 401.
[10] KUCHAŘOVÁ, K.—HORKEL, T.—DLOUHÝ, A.: In: Creep Behavior of Advanced Materials for 21st Century. Eds.: Mishra, R. S., Mukherjee, A. K., Murty, K. L. Warrendale, Pa., TMS 1999, p. 127.

[11] YAWNY, A.—KAUSTRÄTER, G.—SKROTZKI, B.—EGGELER, G.: Scripta Mater., *46*, 2002, p. 837.
[12] MILIČKA, K.—DOBEŠ, F.: J. Alloy Compd., *378*, 2004, p. 167.